DOI: 10.1002/adom.201600483
Article type: Full Paper

Triazolobenzothiadiazole-Based Copolymers for Polymer Light-Emitting Diodes: Pure Near-Infrared Emission via Optimized Energy and Charge Transfer

Petri Murto, Alessandro Minotto, Andrea Zampetti, Xiaofeng Xu, Mats R. Andersson, Franco Cacialli and Ergang Wang**

P. Murto, Dr. X. Xu, Dr. E. Wang
Department of Chemistry and Chemical Engineering/Applied Chemistry
Chalmers University of Technology
SE-412 96 Gothenburg, Sweden
E-mail: ergang@chalmers.se

Dr. A. Minotto, Dr. A. Zampetti, Prof. F. Cacialli
Department of Physics and Astronomy and London Centre for Nanotechnology
University College London
Gower Street, London, WC1E 6BT, UK
E-mail: f.cacialli@ucl.ac.uk

Prof. M. R. Andersson
Future Industries Institute
University of South Australia
Mawson Lakes, South Australia 5095, Australia

Keywords: fluorescent materials, LEDs, near-infrared, polymers

A series of new near-infrared (NIR) emitting copolymers, based on a low band gap 6-(2-butyloctyl)-4,8-di(thiophen-2-yl)-[1,2,3]triazolo[4',5':4,5]benzo[1,2-*c*][1,2,5]thiadiazole (TBTTT) fluorophore copolymerized into a high band gap poly[3,3'-ditetradecyl-2,2'-bithiophene-5,5'-diyl-*alt*-5-(2-ethylhexyl)-4*H*-thieno[3,4-*c*]pyrrole-4,6(5*H*)-dione-1,3-diyl] (P2TTPD) host backbone, for polymer light-emitting diode (PLED) applications is reported. PLEDs fabricated from the host polymer (P2TTPD-0) show external quantum efficiencies (EQEs) up to 0.49% at 690 nm, with turn-on voltage (V_{on}) at only 2.4 V. By incorporating the TBTTT segments into the host polymer backbone, pure NIR emission peaking at ~900 nm is obtained with V_{on} remaining below 5 V. This work demonstrates that such a low V_{on} can be attributed to efficient intrachain energy and/or charge transfer to the TBTTT sites. When the NIR emitting copolymer (P2TTPD-10) is blended with P2TTPD-0, the TBTTT are confined

to well-separated polymer chains. As a result, the EQE from the blend is lower and the V_{on} higher than that obtained from the pure copolymer (P2TTPD-1.0) with equal content of TBTTT. An analogous copolymer (P4T-1.0), consisting of poly[3,3'-ditetradecyl-2,2':5',2":5",2"'-quaterthiophene-5,5"'-diyl] (P4T) as the host and 1% TBTTT as the NIR emitter, further demonstrates that pure NIR emission can be obtained only through optimized molecular orbital energy levels, as in P2TTPD-1.0, which minimizes chances for either charge trapping or exciton splitting.

1. Introduction

Shifting the spectral range of organic light-emitting diodes (OLEDs) from the visible to the near-infrared (NIR) region of the electromagnetic spectrum is of great interest, *e.g.* for security display applications, optical communications and even photodynamic therapy.[1] Recent publications on NIR OLEDs are mostly based on metalloporphyrins[2], rare-earth and transition metal complexes[3], organic small molecules[4] and conjugated polymers.[5] Hybrid organic/inorganic materials referred as Perovskites[6] and nanomaterials such as quantum dots[7] have shown high performance as NIR emitters as well. The two most efficient NIR OLEDs reported to date, based on Pt-porphyrin phosphors, exhibit external quantum efficiency (EQE) of 9.2% at 764 nm and 8.5% at 772 nm.[2a,2c] Polymer light-emitting diodes (PLEDs) based on these phosphors reach EQE of 3.0%, which is among the highest reported for PLEDs. However, such devices are prone to suffer from high turn-on voltage (V_{on}) up to 17 V and, especially for the Pt-OLEDs, significant EQE roll-off at current densities higher than 10^{-3} mA cm^{-2}.[2a-c]

Although a substantial part of the PLEDs research is focused on purely organic (metal-free) fluorescent materials, their efficiencies are still far behind those obtained from the organometallic phosphors.[5b,5c,8] Previously, benzo[*c*][1,2,5]thiadiazole (BT), [1,2,5]thiadiazolo[3,4-*g*]quinoxaline (TQ), benzo[1,2-*c*:4,5-*c'*]bis[1,2,5]thiadiazole (BBT) and

[1,2,3]triazolo[4',5':4,5]benzo[1,2-*c*][1,2,5]thiadiazole (BTT) have been the most commonly used electron deficient units in donor–acceptor–donor (DAD) fluorophores (**Figure 1**).[9] Typically for these materials, both the photoluminescence quantum yield (PLQY) and the EQE decrease with decreasing band gap, due to strong vibronic coupling between the ground and excited states.[10] Strong intermolecular π–π stacking, *i.e.* aggregation, further favors non-radiative decay processes, leading to poor EQE.[8b,8c,11] However, EQEs of ~0.5% with EL peak at ~725 nm from a BT based oligomer and 0.27% at 885 nm and 0.091% at 895 nm from BTT based copolymers reported by some of us are among the best performing NIR PLEDs based on purely organic materials published so far.[9c,12] Despite these promising results, such devices exhibit high V_{on} (11–28 V), as well as high operating voltage (maximum radiance obtained at ~30–50 V).[12] On the other hand, purely organic copolymers can simplify the device fabrication compared for example to the vacuum deposited organometallic small molecules and the use of additional host matrix materials.[13]

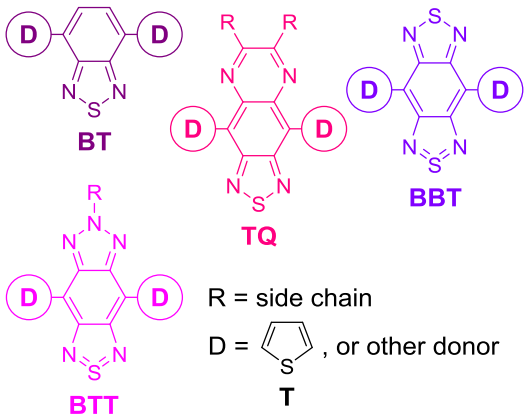

Figure 1. Molecular structures of DAD type NIR emitters BT, TQ, BBT and BTT.

Herein, we present a series of new NIR emitting copolymers based on 6-(2-butyloctyl)-4,8-di(thiophen-2-yl)-[1,2,3]triazolo[4',5':4,5]benzo[1,2-*c*][1,2,5]thiadiazole (TBTTT) as the NIR emitter and poly[3,3'-ditetradecyl-2,2'-bithiophene-5,5'-diyl-*alt*-5-(2-ethylhexyl)-4*H*-thieno[3,4-*c*]pyrrole-4,6(5*H*)-dione-1,3-diyl] (P2TTPD) as the host. As shown in literature,

the amount of NIR emitter is highly related to the EQE of the resulting PLEDs.[8] Therefore, different amounts of TBTTT were copolymerized into the P2TTPD host backbone forming a series of random copolymers (**Figure 2**). We conducted a systematic study on the polymer structure and molecular orbital energy distribution in relation to the optical properties and device performance. An EQE of 0.49% with emission maximum at 690 nm and a V_{on} at only 2.4 V for PLEDs fabricated from P2TTPD-0 were achieved. We obtained pure NIR emission up to 930 nm, yet the V_{on} remaining below 5 V even at 10% TBTTT loading (P2TTPD-10). The polymers did not show EQE roll-offs at increasing current density like those reported for the Pt-porphyrins.[2a,2c] Instead, compared to the Pt-OLEDs,[2a,2c] the maximum EQEs were obtained at about four orders of magnitude higher current density, showing progressive increase from 0.1 up to 10 mA cm^{-2}. Furthermore, we detected emission peaking at 930 nm, *i.e.* more than 100 nm further towards the NIR compared to the aforementioned Pt-porphyrins. The low V_{on} can be attributed to the optimized frontier orbital energy levels, as the highest occupied molecular orbital (HOMO) and lowest unoccupied molecular orbital (LUMO) of the TBTTT NIR unit form a Type I intramolecular heterojunction with the P2TTPD host (Figure 2). This energy levels arrangement enables efficient energy transfer and formation of a low barrier to charge injection in the copolymers. When poly[3,3'-ditetradecyl-2,2':5',2":5",2"'-quaterthiophene-5,5"'-diyl] (P4T) is used as a host in a copolymer P4T-1.0, increased emission component is observed in the visible region. This can be ascribed to a less efficient charge transfer onto the NIR emitter in P4T-1.0 compared to P2TTPD-1.0. Pure NIR emission can be obtained from such donor–weak acceptor–donor–strong acceptor copolymers[8b,8c,12] when the energy and charge transfer work together, allowing efficient energy funnelling and charge trapping at the low-gap NIR fluorophores.

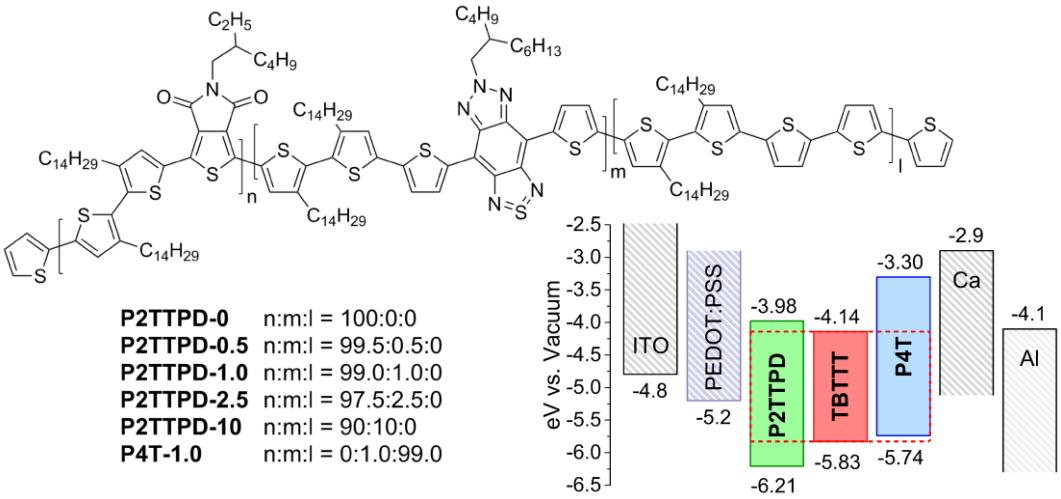

Figure 2. Chemical structures of the polymers P2TTPD-0, P2TTPD-0.5, P2TTPD-1.0, P2TTPD-2.5, P2TTPD-10 and P4T-1.0 and energy level diagram for P2TTPD host, TBTTT NIR unit and P4T host with the device architecture used in this study.

2. Results and Discussion

2.1. Materials

The materials synthesis is described in details in the Supporting Information (Figure S1 and S2). As shown in Figure 2, we added branched *N*-C_4C_6 side chains to TBTTT to reduce the aggregation of the NIR emitting unit and used long *n*-C_{14} side chains on the thiophenes to obtain well-soluble and easily processable polymers. The polymers were synthesized by varying the amount of TBTTT, 5-(2-ethylhexyl)-4*H*-thieno[3,4-*c*]pyrrole-4,6(5*H*)-dione) (TPD), 3,3'-ditetradecyl-2,2'-bithiophene ($2T_R$) and 2,2'-bithiophene (2T) (Figure S2). Both $2T_R$ and 2T are referred as 2T in the polymer names for simplicity. All the monomer amounts are calculated from the initial molar feed ratios and the concentration of the DAD segment is reported as percent (%) with respect to the host throughout this paper. P2TTPD-0.5, P2TTPD-1.0, P2TTPD-2.5 and P2TTPD-10 contain 0.5, 1, 2.5 and 10% of TBTTT as the DAD unit, respectively. Accordingly, P4T-1.0 contains 1% of the DAD. The polymers were end-capped with thiophene, as recent literature shows that this kind of end-capping of the conjugated polymers can significantly improve the charge carrier mobility and the performance of the organic electronics.[14] Number-average molecular weight (M_n) of 10.2 kg mol^{-1}

(polydispersity index, PDI 1.9) was obtained for P2TTPD-0, 9.2 kg mol^{-1} (PDI 2.0) for P2TTPD-0.5, 10.8 kg mol^{-1} (PDI 1.9) for P2TTPD-1.0, 10.4 kg mol^{-1} (PDI 1.8) for P2TTPD-2.5 and 16.7 kg mol^{-1} (PDI 1.7) for P2TTPD-10. We noticed that the M_n increased to 33.4 kg mol^{-1} (PDI 2.2) for P4T-1.0 upon replacing TPD with 2T. This is probably due to higher reactivity of the brominated sites of the electron donating 2T compared to the electron withdrawing TPD. All the polymers show high thermal stability on thermogravimetric analysis. The degradation onset temperature was > 380 °C (Figure S3). No detectable thermal transition was observed on differential scanning calorimetry measurements when heated and cooled over a temperature range of 0–350 °C (Figure S4).

2.2. Molecular Orbital Energy Levels

We used cyclic voltammetry (CV) to determine the HOMO and LUMO levels of the polymers and the TBTTT monomer. The energy levels were estimated from the first oxidation onset potential (E_{ox}) and the first reduction onset potential (E_{red}) relative to the Fc/Fc^+ redox couple (Figure S5). As shown in Figure 2, the HOMO/LUMO of P2TTPD-0 are both deeper than those reported for a similar P2TTPD polymer without any side chains on the 2T donor (–5.43/–3.09 eV).[15] Tail-to-tail alkylation of the 2T moiety in an analogous polymer lowers the LUMO to –3.97 eV, which is in the same level with that of P2TTPD-0.[16] We expect the steric hindrance among the head-to-head side chains to induce torsion to the $2T_R$ sites of the P2TTPD-0 backbone, which lowers the HOMO level, reduces the π–π stacking and promotes amorphous property in the solid state.[17] P2TTPD-0.5, P2TTPD-1.0, P2TTPD-2.5 and P2TTPD-10 have almost identical HOMO/LUMO levels with P2TTPD-0 and no E_{ox}/E_{red} were found for the TBTTT segment using the CV method. This is due to small loading of TBTTT in the polymers and hence relatively small differences in the polymer backbone.[12,18] However, the HOMO/LUMO of the TBTTT monomer are closely inside the band gap of the P2TTPD-0 host (Figure 2). Furthermore, we used $(T_RTPDT_R)_n$ (n = 1, 2, 3) as model

compounds for the P2TTPD host and TBTTT for the DAD unit and optimized the geometries at the density functional theory B3LYP/6-31G(d,p) level.[19] By comparing the HOMO/LUMO of TBTTT with those of $(T_RTPDT_R)_3$, the calculated HOMO and LUMO of TBTTT go inside the $(T_RTPDT_R)_3$ band gap (Table S1, Figure S6 and S7), which is in agreement with the CV results. Such a Type I energy levels arrangement[20] will facilitate efficient energy and charge transfer from the host to the NIR emitter.

This preferred match of the band gaps is not obtained with P4T-1.0 (Figure 2), as the HOMO and LUMO are higher than those of P2TTPD-0 or P2TTPD-1.0. The HOMO of P4T-1.0 is up-lying by approximately 0.1 eV compared to TBTTT, and thus results in an unfavorable Type II alignment.[20] Similar results were obtained by using $(T_RTTT_R)_n$ (n = 1, 2, 3) model compounds for the P4T host. The calculated HOMO of $(T_RTTT_R)_3$ is about 0.1 eV higher than that of TBTTT (Table S1 and Figure S8). In fact, the HOMO/LUMO of P4T-1.0 are close to a plain thiophene polymer such as P3HT and can be addressed solely to the P4T host backbone.[17c] The addition of TPD to the polymer not only changes the LUMO but also lowers the HOMO to a level that reduces the charge injection barrier at the DAD segments (Figure 2) and consequently favors a balanced charge transport to these sites. Moreover, TPD does not act as a charge trap and then does not inhibit charge transport to TBTTT, which would otherwise reduce the NIR emission from the PLEDs.[21]

2.3. Optical Properties

Absorption spectra of the polymer thin films are reported in **Figure 3a**. P2TTPD-0 displays an absorption maximum at 450 nm with an onset of absorption at 628 nm, corresponding to an optical band gap of 1.97 eV. This is slightly narrower than the electrochemical band gap 2.23 eV measured by CV (Figure 2), as the two methods differ in terms of electronic transitions that are measured.[22] Such an absorption band, evident both in the solid state film (Figure 3a) and dilute chloroform solution (Figure S9), is the characteristic of intramolecular charge

transfer (ICT) arising from excitations with the π–π* manifold.[23] P2TTPD-0.5, P2TTPD-1.0, P2TTPD-2.5 and P2TTPD-10 show absorption profiles that are similar to P2TTPD-0 at 450 nm, with an additional ICT π–π* band at ~790 nm. Such additional red-shifted peak is ascribable to a stronger ICT interaction upon incorporating the strong acceptor TBTTT to the polymer backbone, and its intensity increases at increasing TBTTT feed.[24] The absorption onset at ~1000 nm allows us to identify an optical band gap of 1.24 eV. Accordingly, P4T-1.0 shows tiny absorption peak at ~790 nm and the high-energy maximum owed to the host appears at 465 nm, with an onset of absorption at 571 nm. This corresponds to an optical band gap of 2.17 eV for the P4T host and, similarly to P2TTPD-0 discussed earlier, this is slightly narrower than the electrochemical band gap 2.44 eV (Figure 2).

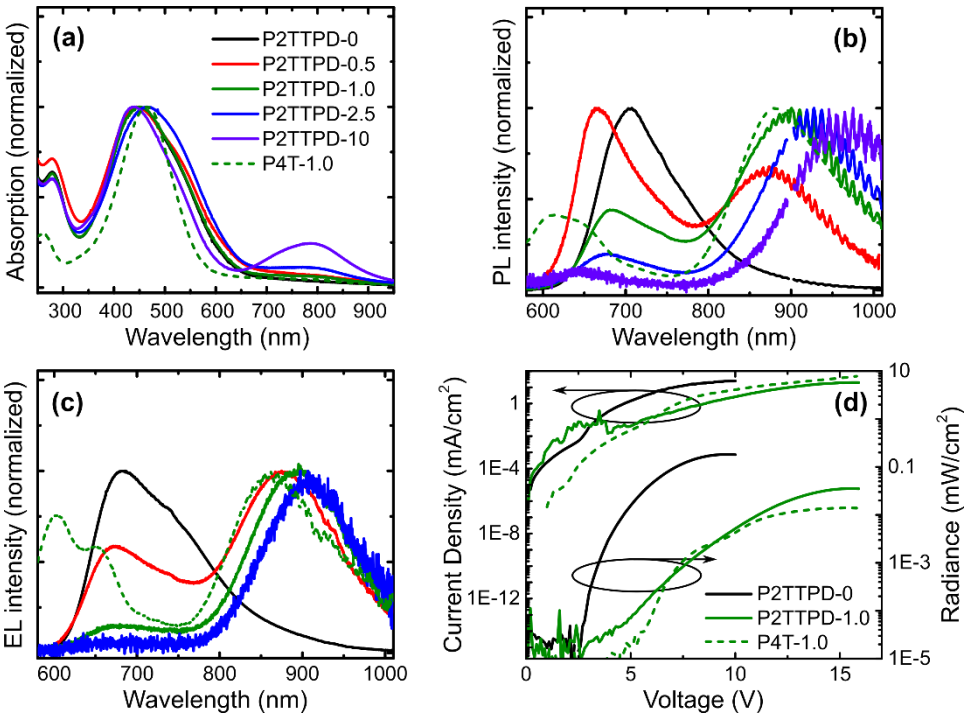

Figure 3. (a) Normalized absorption spectra of polymer thin films (~100 nm) on fused silica glass; (b) Normalized PL of polymers in solid-state thin films. Interference effects at λ > 850 nm are due to optical etaloning inside the CCD camera of the spectrometer; (c) EL of polymers taken at 9 V (P2TTPD-0), 15 V (P2TTPD-0.5) and 16 V (P2TTPD-1.0, P2TTPD-2.5 and P4T-1.0); (d) PLEDs characteristics: current density and radiance versus voltage. The active layer thickness is ~100 nm and the device area is 3.5 mm^2.

The high-energy absorption band of the polymers were almost the same both in thin film and chloroform solution (452 nm, Figure S9). Although the peaks are somewhat broader in films (Figure 3a), this is another proof of the low degree of π–π stacking in the solid state and supports the predicted amorphous property of the head-to-head alkylated polymers. In that perspective, both P2TTPD and P4T can be regarded as suitable host for the NIR emitting TBTTT. However, the low-energy absorption red-shifted from ~740 nm in solution to ~790 nm in film, which indicates stronger ICT interaction induced by closer π–π stacking in the solid state.

In **Figure 3b** the photoluminescence (PL) spectra of the polymers are reported (see Supporting Information for experimental details). P2TTPD-0 show PL peak at 708 nm and PLQY of 20% in solid-state thin films. As expected, the addition of the weak acceptor TPD red-shifted the emission of P2TTPD-0 by ~90 nm compared to polythiophenes such as P3HT, whose reported emission maximum is at ~620 nm.[25] As shown in the Figure 3b, most of the emission lies in the NIR region and, by taking into account the ratio between the photons emitted at $\lambda > 700$ nm and the photons absorbed, we calculated a NIR PLQY of 15%. Since the long PL wavelength of P2TTPD-0 provides almost complete overlap with the absorption of the TBTTT DAD unit, efficient resonant energy transfer (RET) can be expected in the P2TTPD-0.5, P2TTPD-1.0, P2TTPD-2.5 and P2TTPD-10 systems.[8b,8c] Thanks to the RET, we obtained emission in the NIR region from the TBTTT moiety (Figure 3b). By increasing the TBTTT amount from 0.5% to 1, 2.5 and 10% the NIR PL peak red-shifts from 874 nm to 897, 924 and 945 nm, respectively. The red-shift is ascribable to the aggregation of the DADs at increasing concentration, which is well-known for conjugated systems in general and in the specific case of NIR emitting moieties, as reported in previous studies.[8b,8c,12b,18,26] Emission from the host decreases for increasing TBTTT content, but the residual red peak still dominates the PL of P2TTPD-0.5, suggesting that the energy transfer is not complete at 0.5% TBTTT loading. The residual emission from the P2TTPD host backbone appears blue-shifted

by ~40 nm compared to P2TTPD-0 as its low-energy tail is efficiently quenched by the NIR emitting DAD moiety.

We measured the PLQYs for P2TTPD-0.5 (6%) and P2TTPD-1.0 (3%), which exhibit a NIR PLQY of 4% and 3%, respectively. P2TTPD-2.5 and P2TTPD-10 show significantly lower PLQY, probably due to aggregation quenching of the NIR emission. As a result, the NIR PLQY dropped below the 1% sensitivity limit of our experimental setup. In the case of P4T-1.0, the residual PL from P4T host is blue-shifted by ~70 nm compared to the P2TTPD host in P2TTPD-1.0. Despite the poor spectral overlap between the P4T host emission and the TBTTT absorption (Figure 3a and 3b), P4T-1.0 shows PLQY of 5% and NIR PLQY was calculated to be 4%, which is similar to the NIR PLQY obtained from P2TTPD-1.0.

2.4. PLEDs Characterization

PLEDs were fabricated by using the device structure of ITO/PEDOT:PSS anodes and Ca/Al cathodes, according to the procedure described in the Supporting Information. The thickness of the polymer active layer was optimized to ~100 nm. The results of the device characterization are summarized in **Table 1** and the electroluminescence (EL) spectra of the polymers are shown in **Figure 3c**. P2TTPD-0 exhibits an EL maximum at 690 nm, which is ~20 nm blue-shifted compared to the PL spectrum (Figure 3b and 3c). Such blue-shift can be caused by differential charge transfer processes, morphology differences and/or thermochromic effects in the active layer.[27] Moreover, we did not observe any shift in the EL wavelength when the voltage bias was varied by ± 5 V. Nevertheless, the EL is mostly in the NIR region and extending slightly beyond 900 nm. Thanks to the relatively high PLQY, we achieved a maximum EQE of ~0.49% from the device with a maximum radiance of 0.19 mW cm^{-2} (**Figure 3d** and Table 1). The P2TTPD-0 devices show very small EQE roll-offs, thus an EQE of ~0.4% is maintained at currents up to 20 mA cm^{-2}. Furthermore, we found that P2TTPD-0 exhibits V_{on} at only 2.4 V, which is exceptionally low for conjugated

copolymers.[5c,8b,8c,12,28] By considering only the portion of photons emitted at λ > 700 nm, we calculated a NIR EQE of 0.36% for P2TTPD-0. This is among the highest EQEs reported so far in this spectral region and, to the best of our knowledge, the highest NIR EQE reported in literature for a PLED with purely organic (metal-free) copolymer as a single unblended active layer.[5b,5c,9e]

Table 1. Summary of PLEDs performance.

Polymer	TBTTT [%][a)]	Max EQE [%][b)]	NIR EQE [%][c)]	V_{on} [V][d)]	Max Radiance [mW cm^{-2}][e)]	PL peak [nm][f)]	EL peak [nm][f)]
P2TTPD-0	0	0.49 ± 0.12	0.36	2.4 ± 0.3	0.19	708	690
P2TTPD-0.5	0.5	0.15 ± 0.01	0.13	4.3 ± 0.3	0.13	667, 874	680, 880
P2TTPD-1.0	1	0.08 ± 0.05	0.07	4.3 ± 0.6	0.07	681, 897	684, 896
P2TTPD-2.5	2.5	0.010 ± 0.001	0.010	6.4 ± 1.3	0.02	677, 924	909
P2TTPD-10	10	0.004 ± 0.001	0.004	4.6 ± 0.5	0.001	650, 945	930
P4T-1.0	1	0.06 ± 0.01	0.05[h)]	4.7 ± 0.5	0.02	612, 879	604, 864
P2TTPD-10:P2TTPD-0[g)]	1	0.06 ± 0.02	0.06	9.6 ± 1.4	0.01	664, 892	892

[a)]Calculated from the initial feed ratio of the monomers; [b)]Measured at ~10 mA cm^{-2} current density; [c)]Defined as λ > 700 nm; [d)]Intercept of the radiance-voltage curve with the y-axis in a semi-log plot; [e)]Measured at 15 V (at 10 V for P2TTPD-0); [f)]EL and PL maxima at λ > 700 nm correspond to the emission from the DAD moiety, whereas those at λ < 700 nm correspond to the residual emission from the host backbone; [g)]10% w/w blend of P2TTPD-10:P2TTPD-0; [h)]The relative ratio of the visible component varied from pixel to pixel, calculated from the pixel with lowest visible component. All confidence intervals represent the standard deviation between values measured from a minimum of eight devices.

By adding TBTTT to the P2TTPD backbone in P2TTPD-0.5, P2TTPD-1.0 and P2TTPD-2.5 (Figure 3c) the residual emission from the host is quenched more efficiently in the PLEDs compared to the PL experiment (Figure 3b). The NIR EL peak from TBTTT dominates the EL spectra at all concentrations tested in this work. Such a result is indicative of the crucial role of the low band gap NIR moieties in both the charge transport and the mutual polarons capture on these sites, which effectively leads to selective exciton formation at their locations. Although energy transfer from the high band gap host polymer to the NIR moieties (the only active in PL experiments) cannot be ruled out as a mechanism in EL, it is clearly less effective as compared to the former one.[8b,8c,28] We obtained EQE of 0.15% and NIR EQE of 0.13%

with a maximum radiance of 0.13 mW cm^{-2} from P2TTPD-0.5 (Table 1). The emission from the host part becomes more prominent at increasing voltage bias, especially for polymers with small amount of TBTTT. This indicates that the EL from the DAD sites saturates at lower bias compared to the P2TTPD host, thus increasing the rate of exciton formation and recombination at the higher energy sites.[2d]

When the amount of TBTTT was increased to 1% in P2TTPD-1.0 (Figure 3c), the EL maximum red-shifted to 896 nm with a vanishingly small fraction of the emission coming from the host. However, the NIR EQE dropped with the radiance to 0.07% and 0.07 mW cm^{-2}, respectively (Figure 3d and Table 1). Further increase of the TBTTT loading in P2TTPD-2.5 and P2TTPD-10 red-shifts the emission up to 909 and 930 nm, respectively, without any detectable emission from the host (Figure 3c). More DAD sites in the polymer brought the EQE further down and, as a result, we obtained only 0.004% NIR EQE for P2TTPD-10 (Table 1). Similar to the PLQY, the decrease of EQE can be attributed to the aggregation quenching at increasing TBTTT content. However, the devices fabricated from P2TTPD-0.5 and P2TTPD-1.0 are among the most efficient reported in literature for PLEDs emitting at ~900 nm and based on a purely organic active material.[5b,8c,12,29] As for P2TTPD-0, the maximum EQEs of P2TTPD-0.5 and P2TTPD-1.0 (Table 1) are measured at current densities of ~10 mA cm^{-2}. In fact, the EQEs increase with increasing current density from 0.1 to 10 mA cm^{-2} (Figure S10), which is rarely reported for high EQE NIR emitters.[2a-c,3a] As a general trend, we found that the V_{on} of the NIR PLEDs were relatively low (Figure 3d and Table 1). This is an improvement from the high V_{on} at 11–28 V reported previously for the poly[phthalimide-*alt*-thiophene] series with similar concentration of the TBTTT DAD unit.[12] The V_{on} increased slightly with higher concentration of TBTTT, which can be attributed to the increasing amount of the low-gap charge trapping sites in the polymer.

P4T-1.0 exhibits an EL maximum at 864 nm, which is ~30 nm blue-shifted compared to P2TTPD-1.0 (Figure 3c). Furthermore, the visible emission component from the host is higher

and blue-shifted in P4T-1.0 compared to P2TTPD-1.0 and its relative intensity varied substantially between different device samples. The EQE of the devices fabricated from P4T-1.0 was 0.06% (Table 1). It is noteworthy that for P4T-1.0 the EQE roll-off with current density is more pronounced. Moreover, similar to the EL spectra, the EQE profile varies between different samples. The highest NIR EQE of 0.05% was calculated from the spectrum with the lowest visible component, as reported in Table 1. Remarkably, the NIR EQE of P4T-1.0 is at least 30% lower than that of P2TTPD-1.0 and the maximum radiance dropped to 0.02 mW cm^{-2}, which is about 70% lower than that measured for P2TTPD-1.0.

2.5. Study of the Energy and Charge Transfer

As discussed earlier, especially P2TTPD-0.5 and P2TTPD-1.0 show residual PL from the P2TTPD host, indicating incomplete energy transfer. When taking into account the small loading of TBTTT and the limited length of the polymers both in this study (≤ 20 repeating units, except P4T-1.0) and in many previous studies, statistically only few of the polymer chains contain a DAD unit.[8,12b,18,26b] In particular, this is the case in P2TTPD-1.0 (Figure 3b and **Figure 4a**). Hence, the shorter wavelength PL observed from P2TTPD-1.0 originates not only from the pure host polymer without TBTTT, but also from P2TTPD chain segments that are too far from the DAD centers to allow intrachain energy transfer to the NIR emitting moieties.[21c,30] This can be due to the low concentration of the DAD segments and the long side chains, which both control the average intermolecular distance. On the other hand, the host emission is quenched almost completely in the EL spectra, as in this case injected charges can migrate more easily from one chain to another, ultimately favoring the exciton formation and recombination at the lowest-gap sites.

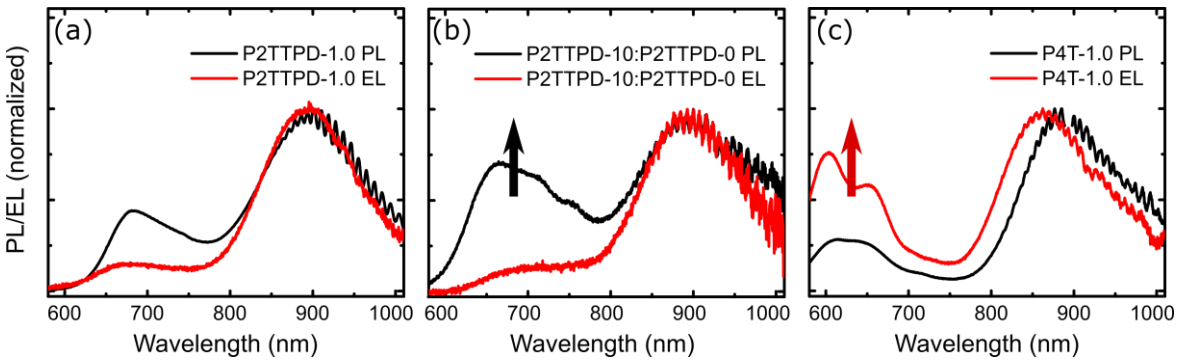

Figure 4. Comparison between normalized PL (black lines) and EL (red lines) spectra of (a) P2TTPD-1.0, (b) P2TTPD-10:P2TTPD-0 blend and (c) P4T-1.0. Arrows are to highlight the increase of the host emission with respect to the PL and EL of P2TTPD-1.0.

To have a clearer view of which one is the dominant transport process, we prepared a 10% w/w blend of P2TTPD-10 in P2TTPD-0 host to obtain 1% total concentration of the DAD segment in the blend (P2TTPD-10:P2TTPD-0), similarly to P2TTPD-1.0. Such a blend increases the amount of P2TTPD host chains, leading to a segregation of the P2TTPD-10 chains within the host matrix and thereby increase of the average distance between the host and DAD moieties. As illustrated in **Figure 4b**, the blend shows a PL maximum at 892 nm, which is ~50 nm blue-shifted compared to P2TTPD-10 (Figure 3b and Table 1) and match the NIR PL peak of P2TTPD-1.0 due to reduced DAD aggregation (Figure 4a). The PLQY of the blend is 4%, which is also close to the value obtained for P2TTPD-1.0. However, as illustrated in Figure 4a and 4b, the intensity of the residual emission from the host is higher for the blend and hence the relative portion of the NIR emission from the DAD sites is lower compared to the PL of P2TTPD-1.0. Such less efficient quenching of the P2TTPD host emission can be ascribed to a reduced intrachain energy transfer (more active in P2TTPD-1.0), as in the case of blend far less than 10% of the polymer chains contain the low band gap DAD moiety.

In addition, we measured the PL decay transient at the emission maximum of P2TTPD host at 680 nm for P2TTPD-0, P2TTPD-1.0 and P2TTPD-10:P2TTPD-0 blend (**Figure 5**). The PL decay of P2TTPD-0 can be fitted with a mono-exponential function with 1.50 ns time constant. Both the blend and P2TTPD-1.0 exhibit a drop in the lifetime and show a bi-

exponential behaviour. The PL decay is dominated by a fast component whose lifetime is < 100 ps, *i.e.* below our instrument response function. Such fast component is due to energy transfer to the DAD sites and comes with an amplitude of 80% for P2TTPD-1.0 and 65% for the blend. This results in a slightly slower recombination process for the blend (Figure 5, red line) as interchain energy transfer is less efficient than intrachain energy transfer. On the other hand, as shown in the EL spectra for both P2TTPD-1.0 and blend (Figure 4a and 4b) the host emission was almost completely quenched when it comes to PLEDs due to an efficient charge transfer. As mentioned before, when a voltage bias is applied, injected charges efficiently migrate through the polymer layer and are ultimately trapped at the low-gap DAD sites. The EL spectrum of the blend device is peaked at 892 nm, similarly to P2TTPD-1.0, with an EQE of 0.06%. Such value coincides with the one obtained from P2TTPD-1.0 if the confidence interval is considered (Table 1). However, the radiance dropped down to 0.01 mW cm^{-2}, which is about 85% lower than that of P2TTPD-1.0. This indicates that although the host emission is efficiently quenched in both devices, fewer radiative excitons are generated in the energy/charge transfer processes in the blend compared to the pure copolymer. Another clear difference that can be noticed in Table 1 is the average V_{on} at 9.6 V for the blend, which is more than two times higher than the one obtained from P2TTPD-1.0 devices. This substantial increase of the V_{on} must be related to an increase of the energetic barrier necessary to inject charges in the device.[31] As mentioned before, the low band gap moieties, *i.e.* charge trap states, are confined in well-separated polymer chains in the blend, which probably affects the injection and transport properties of the active layer.

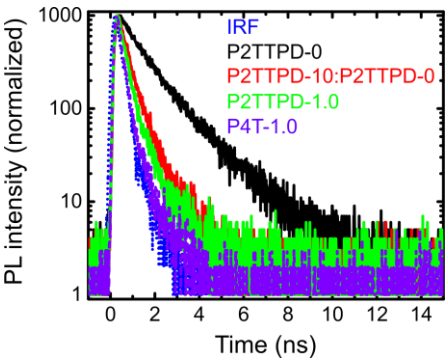

Figure 5. PL decay transients for thin films (100 nm thick on fused silica glass) of P2TTPD-0, P2TTPD-1.0 and P2TTPD-10:P2TTPD-0 blend taken at 680 nm and P4T-1.0 at 610 nm, following excitation at 371 nm. The instrument response function (IRF) is also reported.

The PL and EL spectra of P4T-1.0 are reported in **Figure 4c** for comparison. The DAD content in the P4T-1.0 active layer is the same as in P2TTPD-1.0 but in this case TPD is not present. As discussed earlier, the HOMO and LUMO of the TBTTT segment are not completely encompassed by those of the P4T host and the emission of P4T does not overlap with the absorption of the DAD moiety (Figure 2 and 3). Therefore, both unbalanced charge injection and poor energy transfer are expected in P4T-1.0. However, the PL from P4T is efficiently quenched, similar to P2TTPD-1.0 (Figure 4a and 4c), and the PL decay lifetime is even faster and below the detection limit of our instrument (Figure 5). Since RET can be reasonably ruled out as the dominant mechanism because of the poor spectral overlap, such quenching can be ascribed then only to Dexter energy transfer, which does not require dipole-dipole coupling and mostly relies on the wave function overlap between the donor and acceptor.[32] This is significant only at very short distances (~10 Å) and, given the low degree of π–π stacking of the solid-state film (*vide infra*), this also tells us that intrachain Dexter energy transfer from the P4T donor to the DAD units is the dominating quenching process. The host emission from P4T-1.0 becomes more prominent when moving to the EL spectrum (Figure 4c). In the case of EL, the exciton generation is influenced by different mobility of injected holes and electrons in the polymer. In particular, injected holes tend to hop through P4T regions, given the higher-lying HOMO compared to that of TBTTT (Figure 2).

This result, together with lower EQE and PLED radiance and slightly higher V_{on} shown in Table 1, demonstrates the importance of the addition of TPD into the host polymer backbone. First of all, although the HOMO of TBTTT is similar to the P4T host, its low-lying LUMO can function as a trap for the injected electrons (a potential barrier of about 0.8 V exists, Figure 2), lowering the barrier height for hole injection at the TBTTT sites.[21c,31,33] Despite this, the less efficient quenching of the host EL in P4T-1.0 compared to P2TTPD-1.0 and P2TTPD-10:P2TTPD-0 blend indicates that the charge transfer alone does not allow us to obtain pure NIR EL via P4T host (Figure 4). On the other hand, the addition of TPD also brings down the HOMO to a level that is favorable for balanced energy and charge transfer to the lowest energy sites and enables formation of a Type I (instead of Type II) intramolecular heterojunction.[20] This in turn leads to higher efficiency and radiance from P2TTPD-1.0 over the P4T-1.0 devices.

3. Conclusion

In summary, we have synthesized and characterized a series of new copolymers based on a high band gap P2TTPD host containing different amount of a low band gap TBTTT DAD unit as a NIR emitter. PLEDs fabricated from P2TTPD-0 exhibit EQE of 0.49% at 690 nm and maximum radiance of 0.19 mW cm^{-2}, with V_{on} at 2.4 V. Pure NIR emission up to 930 nm is obtained by incorporating the DAD segment into the P2TTPD backbone. The polymer with 0.5% TBTTT (P2TTPD-0.5) shows the best NIR EQE (0.13%) and radiance (0.13 mW cm^{-2}), with V_{on} at 4.3 V. The V_{on} remained below 5 V at 10% TBTTT loading (P2TTPD-10). The devices reach maximum efficiency below 15 V and exhibit very small EQE roll-offs at increasing current density, up to 20 mA cm^{-2}. We demonstrated that efficient energy transfer is crucial for obtaining high EQE and radiance, yet low V_{on} from the study on PLEDs by blending the NIR copolymer P2TTPD-10 with P2TTPD-0 host, *i.e.* by increasing the intermolecular distance between the host and DAD segments. Furthermore, optimized

HOMO/LUMO levels of the host (P2TTPD) with respect to the TBTTT unit enables balanced electron/hole transfer and minimizes chances for exciton splitting, which is demonstrated with another polymer P4T-1.0. In this unbalanced system, particularly due to the high-lying HOMO of P4T host, increased emission component in the visible is observed. Pure NIR emission is obtained via P2TTPD host due to efficient energy and charge transfer and exciton formation at the TBTTT sites. Devices reported in this study are among the best performing NIR PLEDs based on purely organic (metal-free) copolymers and among the few materials emitting in the ~900 nm region.

Supporting Information

Detailed information on synthetic procedures and polymer characterization including TGA, DSC and CV, together with calculation, PL and PLQY measurements and PLEDs fabrication and characterization.

Supporting Information is available online from the Wiley Online Library or from the author.

Acknowledgements

P.M. and A.M. contributed equally to this work. The authors gratefully acknowledge funding from the European Community's Seventh Framework Programme (FP7/2007-2013) under Grant Agreement No. 607585 (OSNIRO), the Swedish Research Council, the Swedish Research Council Formas, and Chalmers Area of Advance Materials Science and Energy. F.C. is a Royal Society Wolfson Merit Award holder.

Received: ((will be filled in by the editorial staff))
Revised: ((will be filled in by the editorial staff))
Published online: ((will be filled in by the editorial staff))

[1] a) J. Fischer, M. Tietke, F. Fritze, O. Muth, M. Paeschke, D. Han, J. Kwack, T. Kim, J. Lee, S. Kim, H. Chung, *J. Soc. Inf. Display* **2011**, *19*, 163; b) P. A. Haigh, F. Bausi, Z. Ghassemlooy, I. Papakonstantinou, H. Le Minh, C. Flechon, F. Cacialli, *Opt. Express* **2014**, *22*, 2830; c) P. A. Haigh, F. Bausi, H. Le Minh, I. Papakonstantinou, W. O. Popoola, A. Burton, F. Cacialli, *IEEE J. Sel. Areas Commun.* **2015**, *33*, 1819; d) Z. Meng, F. Wei, R. Wang, M. Xia, Z. Chen, H. Wang, M. Zhu, *Adv. Mater.* **2016**, *28*, 245.

[2] a) Y. Sun, C. Borek, K. Hanson, P. I. Djurovich, M. E. Thompson, J. Brooks, J. J. Brown, S. R. Forrest, *Appl. Phys. Lett.* **2007**, *90*, 213503; b) J. R. Sommer, R. T. Farley, K. R. Graham, Y. Yang, J. R. Reynolds, J. Xue, K. S. Schanze, *ACS Appl. Mater. Interfaces* **2009**, *1*, 274; c) K. R. Graham, Y. Yang, J. R. Sommer, A. H. Shelton, K. S. Schanze, J. Xue, J. R. Reynolds, *Chem. Mater.* **2011**, *23*, 5305; d) O. Fenwick, J. K. Sprafke, J. Binas, D. V. Kondratuk, F. Di Stasio, H. L. Anderson, F. Cacialli, *Nano Lett.* **2011**, *11*, 2451.

[3] a) J.-L. Liao, Y. Chi, C.-C. Yeh, H.-C. Kao, C.-H. Chang, M. A. Fox, P. J. Low, G.-H. Lee, *J. Mater. Chem. C* **2015**, *3*, 4910; b) L. Y. Zhang, Y. J. Hou, M. Pan, L. Chen, Y. X. Zhu, S. Y. Yin, G. Shao, C. Y. Su, *Dalton Trans.* **2015**, *44*, 15212; c) X. Cao, J. Miao, M. Zhu, C. Zhong, C. Yang, H. Wu, J. Qin, Y. Cao, *Chem. Mater.* **2015**, *27*, 96.

[4] a) L. Yao, S. Zhang, R. Wang, W. Li, F. Shen, B. Yang, Y. Ma, *Angew. Chem. Int. Ed. Engl.* **2014**, *53*, 2119; b) S. Wang, X. Yan, Z. Cheng, H. Zhang, Y. Liu, Y. Wang, *Angew. Chem. Int. Ed. Engl.* **2015**, *54*, 13068; c) X. Han, Q. Bai, L. Yao, H. Liu, Y. Gao, J. Li, L. Liu, Y. Liu, X. Li, P. Lu, B. Yang, *Adv. Funct. Mater.* **2015**, *25*, 7521; d) P. Ledwon, P. Zassowski, T. Jarosz, M. Lapkowski, P. Wagner, V. Cherpak, P. Stakhira, *J. Mater. Chem. C* **2016**, *4*, 2219.

[5] a) G. Tzamalis, V. Lemaur, F. Karlsson, P. O. Holtz, M. Andersson, X. Crispin, J. Cornil, M. Berggren, *Chem. Phys. Lett.* **2010**, *489*, 92; b) P. Li, O. Fenwick, S. Yilmaz, D. Breusov, D. J. Caruana, S. Allard, U. Scherf, F. Cacialli, *Chem. Commun.* **2011**, *47*, 8820; c) X. Gao, B. Hu, G. Tu, *Org. Electron.* **2014**, *15*, 1440.

[6] J. Wang, N. Wang, Y. Jin, J. Si, Z. K. Tan, H. Du, L. Cheng, X. Dai, S. Bai, H. He, Z. Ye, M. L. Lai, R. H. Friend, W. Huang, *Adv. Mater.* **2015**, *27*, 2311.

[7] A. K. Bansal, F. Antolini, S. Zhang, L. Stroea, L. Ortolani, M. Lanzi, E. Serra, S. Allard, U. Scherf, I. D. W. Samuel, *J. Phys. Chem. C* **2016**, *120*, 1871.

[8] a) M. Sun, X. Jiang, W. Liu, T. Zhu, F. Huang, Y. Cao, *Synth. Met.* **2012**, *162*, 1406; b) O. Fenwick, S. Fusco, T. N. Baig, F. Di Stasio, T. T. Steckler, P. Henriksson, C. Fléchon, M. R. Andersson, F. Cacialli, *APL Mater.* **2013**, *1*, 032108; c) T. T. Steckler, O. Fenwick, T. Lockwood, M. R. Andersson, F. Cacialli, *Macromol. Rapid Commun.* **2013**, *34*, 990.

[9] a) S. Kato, T. Matsumoto, T. Ishi-i, T. Thiemann, M. Shigeiwa, H. Gorohmaru, S. Maeda, Y. Yamashita, S. Mataka, *Chem. Commun.* **2004**, 2342; b) G. Qian, B. Dai, M. Luo, D. Yu, J. Zhan, Z. Zhang, D. Ma, Z. Y. Wang, *Chem. Mater.* **2008**, *20*, 6208; c) S. Ellinger, K. R. Graham, P. Shi, R. T. Farley, T. T. Steckler, R. N. Brookins, P. Taranekar, J. Mei, L. A. Padilha, T. R. Ensley, H. Hu, S. Webster, D. J. Hagan, E. W. Van Stryland, K. S. Schanze, J. R. Reynolds, *Chem. Mater.* **2011**, *23*, 3805; d) D. G. Patel, F. Feng, Y. Y. Ohnishi, K. A. Abboud, S. Hirata, K. S. Schanze, J. R. Reynolds, *J. Am. Chem. Soc.* **2012**, *134*, 2599; e) Y. Zhang, X. Gao, J. Li, G. Tu, *Dyes Pigm.* **2015**, *120*, 112.

[10] a) J. V. Caspar, E. M. Kober, B. P. Sullivan, T. J. Meyer, *J. Am. Chem. Soc.* **1982**, *104*, 630; b) Z. R. Grabowski, K. Rotkiewicz, *Chem. Rev.* **2003**, *103*, 3899.

[11] G. Tregnago, C. Fléchon, S. Choudhary, C. Gozalvez, A. Mateo-Alonso, F. Cacialli, *Appl. Phys. Lett.* **2014**, *105*, 143304.

[12] a) T. T. Steckler, M. J. Lee, Z. Chen, O. Fenwick, M. R. Andersson, F. Cacialli, H. Sirringhaus, *J. Mater. Chem. C* **2014**, *2*, 5133; b) G. Tregnago, T. T. Steckler, O. Fenwick, M. R. Andersson, F. Cacialli, *J. Mater. Chem. C* **2015**, *3*, 2792.

[13] a) D.-Y. Chung, J. Huang, D. D. C. Bradley, A. J. Campbell, *Org. Electron.* **2010**, *11*, 1088; b) C. Zhong, C. Duan, F. Huang, H. Wu, Y. Cao, *Chem. Mater.* **2011**, *23*, 326; c) M. Shibata, Y. Sakai, D. Yokoyama, *J. Mater. Chem. C* **2015**, *3*, 11178; d) K. Gilissen, J.

Stryckers, P. Verstappen, J. Drijkoningen, G. H. L. Heintges, L. Lutsen, J. Manca, W. Maes, W. Deferme, *Org. Electron.* **2015**, *20*, 31; e) N. Thejo Kalyani, S. J. Dhoble, *Renew. Sust. Energy Rev.* **2015**, *44*, 319.

[14] a) J. K. Park, J. Jo, J. H. Seo, J. S. Moon, Y. D. Park, K. Lee, A. J. Heeger, G. C. Bazan, *Adv. Mater.* **2011**, *23*, 2430; b) S. Kim, J. K. Park, Y. D. Park, *RSC Adv.* **2014**, *4*, 39268; c) U. Koldemir, S. R. Puniredd, M. Wagner, S. Tongay, T. D. McCarley, G. D. Kamenov, K. Müllen, W. Pisula, J. R. Reynolds, *Macromolecules* **2015**, *48*, 6369.

[15] D. Chen, Y. Zhao, C. Zhong, S. Gao, G. Yu, Y. Liu, J. Qin, *J. Mater. Chem.* **2012**, *22*, 14639.

[16] S. Beaupré, A. Pron, S. H. Drouin, A. Najari, L. G. Mercier, A. Robitaille, M. Leclerc, *Macromolecules* **2012**, *45*, 6906.

[17] a) S. Ko, E. T. Hoke, L. Pandey, S. Hong, R. Mondal, C. Risko, Y. Yi, R. Noriega, M. D. McGehee, J. L. Bredas, A. Salleo, Z. Bao, *J. Am. Chem. Soc.* **2012**, *134*, 5222; b) X. Guo, J. Quinn, Z. Chen, H. Usta, Y. Zheng, Y. Xia, J. W. Hennek, R. P. Ortiz, T. J. Marks, A. Facchetti, *J. Am. Chem. Soc.* **2013**, *135*, 1986; c) J.-S. Kim, J.-H. Kim, W. Lee, H. Yu, H. J. Kim, I. Song, M. Shin, J. H. Oh, U. Jeong, T.-S. Kim, B. J. Kim, *Macromolecules* **2015**, *48*, 4339.

[18] L. Zhang, S. Hu, J. Chen, Z. Chen, H. Wu, J. Peng, Y. Cao, *Adv. Funct. Mater.* **2011**, *21*, 3760.

[19] a) W. J. Hehre, *J. Chem. Phys.* **1972**, *56*, 2257; b) J. P. Perdew, Y. Wang, *Phys. Rev. B* **1992**, *45*, 13244; c) A. D. Becke, *J. Chem. Phys.* **1993**, *98*, 5648; d) A. J. Cohen, P. Mori-Sanchez, W. Yang, *Chem. Rev.* **2012**, *112*, 289.

[20] a) E. R. Bittner, J. G. Ramon, S. Karabunarliev, *J. Chem. Phys.* **2005**, *122*, 214719; b) Y.-S. Huang, S. Westenhoff, I. Avilov, P. Sreearunothai, J. M. Hodgkiss, C. Deleener, R. H. Friend, D. Beljonne, *Nat. Mater.* **2008**, *7*, 483.

[21] a) C.-C. Wu, J. C. Sturm, R. A. Register, J. Tian, E. P. Dana, M. E. Thompson, *IEEE Trans. Electron Devices* **1997**, *44*, 1269; b) V. Cleave, G. Yahioglu, P. Le Barny, D.-H. Hwang, A. B. Holmes, R. H. Friend, N. Tessler, *Adv. Mater.* **2001**, *13*, 44; c) X. Gong, J. C. Ostrowski, D. Moses, G. C. Bazan, A. J. Heeger, *Adv. Funct. Mater.* **2003**, *13*, 439.

[22] X. Xu, C. Wang, O. Bäcke, D. I. James, K. Bini, E. Olsson, M. R. Andersson, M. Fahlman, E. Wang, *Polym. Chem.* **2015**, *6*, 4624.

[23] a) L. Zaikowski, G. Mauro, M. Bird, B. Karten, S. Asaoka, Q. Wu, A. R. Cook, J. R. Miller, *J. Phys. Chem. B* **2015**, *119*, 7231; b) E. N. Hooley, D. J. Jones, N. C. Greenham, K. P. Ghiggino, T. D. M. Bell, *J. Phys. Chem. B* **2015**, *119*, 7266; c) Z. Li, X. Xu, W. Zhang, X. Meng, W. Ma, A. Yartsev, O. Inganas, M. R. Andersson, R. A. J. Janssen, E. Wang, *J. Am. Chem. Soc.* DOI: 10.1021/jacs.6b04822.

[24] a) H. Zhou, L. Yang, S. Stoneking, W. You, *ACS Appl. Mater. Interfaces* **2010**, *2*, 1377; b) X. Lu, S. Fan, J. Wu, X. Jia, Z.-S. Wang, G. Zhou, *J. Org. Chem.* **2014**, *79*, 6480.

[25] a) Y. Kim, D. D. C. Bradley, *Curr. Appl. Phys.* **2005**, *5*, 222; b) M. Valadares, I. Silvestre, H. D. R. Calado, B. R. A. Neves, P. S. S. Guimarães, L. A. Cury, *Mater. Sci. Eng., C* **2009**, *29*, 571.

[26] a) S. Brovelli, G. Latini, M. J. Frampton, S. O. McDonnell, F. E. Oddy, O. Fenwick, H. L. Anderson, F. Cacialli, *Nano Lett.* **2008**, *8*, 4546; b) A. Petrozza, S. Brovelli, J. J. Michels, H. L. Anderson, R. H. Friend, C. Silva, F. Cacialli, *Adv. Mater.* **2008**, *20*, 3218.

[27] a) G. Latini, A. Downes, O. Fenwick, A. Ambrosio, M. Allegrini, C. Daniel, C. Silva, P. G. Gucciardi, S. Patanè, R. Daik, W. J. Feast, F. Cacialli, *Appl. Phys. Lett.* **2005**, *86*, 011102; b) E. Tekin, D. A. M. Egbe, J. M. Kranenburg, C. Ulbricht, S. Rathgeber, E. Birckner, N. Rehmann, K. Meerholz, U. S. Schubert, *Chem. Mater.* **2008**, *20*, 2727; c) R. Noriega, J. Rivnay, K. Vandewal, F. P. V. Koch, N. Stingelin, P. Smith, M. F. Toney, A. Salleo, *Nat. Mater.* **2013**, *12*, 1038.

[28] D. Cao, Q. Liu, W. Zeng, S. Han, J. Peng, S. Liu, *Macromolecules* **2006**, *39*, 8347.

[29] M. Chen, E. Perzon, M. R. Andersson, S. Marcinkevicius, S. K. M. Jönsson, M. Fahlman, M. Berggren, *Appl. Phys. Lett.* **2004**, *84*, 3570.

[30] T. Förster, *Discuss. Faraday Soc.* **1959**, *27*, 7.

[31] a) D. F. O'Briena, C. Giebelerb, R. B. Fletcherb, A. J. Cadbyb, L. C. Palilisb, D. G. Lidzeyb, P. A. Laneb, D. D. C. Bradleyb, W. Blau, *Synth. Met.* **2001**, *116*, 379; b) H. Wu, F. Huang, Y. Mo, W. Yang, D. Wang, J. Peng, Y. Cao, *Adv. Mater.* **2004**, *16*, 1826; c) H. A. Al Attar, A. P. Monkman, *Adv. Funct. Mater.* **2006**, *16*, 2231.

[32] a) H. A. Al Attar, A. P. Monkman, M. Tavasli, S. Bettington, M. R. Bryce, *Appl. Phys. Lett.* **2005**, *86*, 121101; b) F. B. Dias, M. Knaapila, A. P. Monkman, H. D. Burrows, *Macromolecules* **2006**, *39*, 1598.

[33] J. J. M. Halls, J. Cornil, D. A. dos Santos, R. Silbey, D.-H. Hwang, A. B. Holmes, J. L. Brédas, R. H. Friend, *Phys. Rev. B* **1999**, *60*, 5721.

Near-infrared polymer light-emitting diodes (NIR PLEDs) are fabricated from a series of conjugated copolymers. Triazolobenzothiadiazole is used as a low band gap NIR fluorophore, which is copolymerized in small quantities into a high band gap host polymer backbone. Pure NIR emission is obtained by optimizing both charge and energy transfer to the low-gap sites.

Keywords: fluorescent materials, LEDs, near-infrared, polymers

P. Murto, A. Minotto, A. Zampetti, X. Xu, M. R. Andersson, F. Cacialli and E. Wang

Triazolobenzothiadiazole-Based Copolymers for Polymer Light-Emitting Diodes: Pure Near-Infrared Emission via Optimized Energy and Charge Transfer